

Study of Silicon Photomultiplier Radiation Hardness with the JULIC Cyclotron

T. Tolba^{a,1,2} D. Grzonka^{a,1} T. Seifick^a J. Ritman^a

^a*Institut für Kernphysik, Forschungszentrum Jülich, 52428 Jülich, Germany*

ABSTRACT: In this work we study the performance of silicon photomultiplier (SiPM) light sensors after exposure to the JULIC cyclotron proton beam, of energy ~ 35 MeV, relative to their performance in the absence of an exposure. The SiPM devices used in this study show a significant change in their behavior and relatively large shift towards lower values, by up to ~ 2 V, in their breakdown voltage. The SiPMs are found to be no longer usable for single photon measurements after being exposed to radiation dose of ~ 0.2 Gy (corresponding to an integrated proton flux of $\sim \phi_p = 9.6 \times 10^7$ p/cm²). No visible damage to the surface of the devices was caused by the exposure.

KEYWORDS: Proton beam, Cyclotron, Radiation hardness, Photon detectors for UV, visible and IR photons (solid-state), SiPM, Absorbtion dose

ARXIV EPRINT:

¹Corresponding author

²Now at the Institut für Experimentalphysik, University of Hamburg, 22761 Hamburg, Germany

1	Introduction	1
2	Instrumentation	4
2.1	The Test Setup	4
2.2	The Photo-Sensors	4
2.3	The Data Acquisition (DAQ) System and Data Collection	5
3	Data Analysis	5
3.1	I-V Curve Studies	7
3.2	SiPM Performance with Light	7
3.3	SiPMs Visual Inspection	8
4	Data Taking During Irradiation	9
4.1	Relative Gain	11
4.2	Relative Dark Current Rate	11
4.3	Prompt Cross-Talk Probability	12
4.4	Delayed Correlated Noise Probability	12
5	Conclusions	14

1 Introduction

Silicon photomultipliers (SiPMs) are multi-pixel semiconductor devices, with pixels (microcells) arranged on a common silicon substrate. Each microcell is a Geiger-mode avalanche photodiode (GM-APD), working above the breakdown voltage (U_{bd}), and it has a resistor for passive quenching of the breakdown. SiPMs are designed to have high gain (typically $\sim 10^6$), high photon detection efficiency (PDE) [1], excellent time resolution, and wide range spectral response. They can be used to detect light signals at the single photon level. Compared with traditional photomultiplier tubes (PMTs), SiPMs are insensitive to the external magnetic field, more compact and do not require high operating voltage. These features make SiPMs very attractive photosensors for experiments where excellent particle detection is a key parameter.

As an example of an experiment that intends to use SiPMs as photosensors to detect fast scintillation light is the barrel time of flight (barrel-ToF) detector [2] of the future \bar{P} ANDA spectrometer at FAIR in Darmstadt, Germany [3]. The barrel-ToF detector will be located at ~ 50 cm radial distance to the beam axis. This location exposes the barrel-ToF to high radiation levels. It is thus imperative to avoid severe degradation of the SiPMs' performance due to this exposure. The estimated average equivalent neutron dose on the barrel-ToF detector is in order of $\sim 9.13 \times 10^9 n_{eq}(1 \text{ MeV})/\text{cm}^2$ a year [2] (the equivalent neutron dose can be calculated by multiplying the proton flux, ϕ_P , by the hardness factor, κ , of Silicon, which depends on the proton energy and can be deduced from [4]). This estimated neutron equivalent flux is based on assuming fused silica material. Because the

exact internal structure and doping concentrations of the SiPMs are not disclosed by vendors, it is difficult to accurately estimate/simulate a priori the effect of the radiation damage on the SiPM structure. Thus, the radiation dependence, as a function of energy and flux, of such devices must be measured experimentally.

The expected damage effect from the radiation exposure can be categorized, depending on the energy loss process due to the interaction between the impinging radiation and the SiPM tile [5], as follows:

1. Surface damage due to the Ionizing Energy Loss (IEL) process, which is usually caused by photons and light charged particles, e.g. electrons. The surface damage of the SiPM tiles can cause:
 - (a) Charge build-up on the surface-protection Oxide layer of the SiPM.
 - (b) Increase in the leakage current of the SiPM.
2. Bulk damage due to the Non-Ionizing Energy Loss (NIEL) process, which is usually caused by heavier particles, e.g. protons, neutrons and pions. The bulk damage of a SiPM can cause:
 - (a) Crystal defects in the bulk of the Si lattice. This is usually generated by the heavy particles that penetrate in the bulk of the SiPM die and cause a mono-/multi-displacement of the Si atoms (the Primary Knock-on Atoms (PKA)).
 - (b) Change of effective doping concentration by producing acceptor like defects which modify the depletion (breakdown) voltage.
 - (c) Increase of charge carrier trapping which leads to a loss of charge (signal),
 - (d) Increase of the gain due to the change in the breakdown voltage.
 - (e) Easier thermal excitement of electrons and holes that causes an increase of the leakage current, hence the dark current noise.

Numerous experimental investigations have been conducted to study the influence of proton radiation exposure on the performance of the SiPMs [6–12] (the effects of radiation damage in SiPMs due to other heavy particles, e.g. neutrons, and gammas can be found in [13, 14]). However, the results from the different studies are found to be not consistent with each other, especially on the operational conditions of the SiPMs after exposure to high and low fluxes. Table 1, summarizes the previous work on SiPMs radiation hardness studies with protons, which mostly were conducted at energies lower than 212 MeV [6–10, 12]. There is only one measurement at very high energy, 23 GeV [11]. Comparing different measurements in Table 1 requires non-trivial assumptions and there is ambiguity in interpreting data, which supports our claim for the importance of an experimental measurement.

A first step of these studies is the irradiation test of the SiPMs at low energy, in order to understand the performance of these devices at their fundamental working conditions, i.e. in the dark and at room temperature, which is covered in this paper. These studies will be continued with light conditions and with higher proton momenta up to about 3 GeV/c, an energy region more relevant for experiments like the PANDA experiment for which no previous studies of SiPMs concerning radiation hardness were performed.

Table 1: Summary of existing studies on SiPMs radiation hardness. For each study the table shows the proton energy used in the study E_p , proton fluence (ϕ_p), the 1 MeV neutron equivalent fluence (ϕ_{n-eq}) and the absorption dose (**Dose**).

Reference	E_p [MeV]	ϕ_p [P/cm ²]	ϕ_{n-eq} [n _{eq} /cm ²]	Dose [Gy]	Main Results
Heering [6] (2008)	212	3.00x10 ¹³	8.00x10 ¹²	1.68x10 ⁴	<ul style="list-style-type: none"> - Increase in leakage current - Increase in dark count rate - Decrease in gain - At max. ϕ_p SiPM are not working
Musienko [7] (2009)	83	1.00x10 ¹⁰	2.00x10 ¹⁰	1.05x10 ¹	<ul style="list-style-type: none"> - Increase in leakage current - Increase in dark count rate - No change in U_{bd} and R_q - Reduction in PDE (< 10%) - Reduction in gain (> 10%)
Bohn [8] (2009)	212	3.00x10 ¹⁰	2.40x10 ¹⁰	1.68x10 ¹	<ul style="list-style-type: none"> - Increase in leakage current - Increase in dark noise - At max. ϕ_p SiPMs are working - Reduction in PDE (4% - 49%)
Matsumura [9] (2009)	53.3	2.80x10 ¹⁰	4.80x10 ¹⁰	4.20x10 ¹	<ul style="list-style-type: none"> - Increase in leakage current - No significant change in gain - At 21 Gy no photon counting - Pulse height reduced at 42 Gy
Heering [11] (2014)	62	6.00x10 ¹²	1.20x10 ¹³	8.02x10 ³	<ul style="list-style-type: none"> - Increase in dark current - 200 mV shift in U_{bd}
Musienko [10] (2015)	62	1.00x10 ¹²	2.00x10 ¹²	1.34x10 ³	<ul style="list-style-type: none"> - Increase in leakage current - Increase in dark noise - 178 mV shift in U_{bd} - Reduction in gain (< 38%)
Heering [11] (2016)	23000	1.30x10 ¹⁴	2.20x10 ¹⁴		<ul style="list-style-type: none"> - Increase in dark noise - ~ 4 V shift in U_{bd} - Reduction in PDE by 25% - At max. ϕ_p SiPMs are working
Lacombe [12] (2019)	10 49.7	7x10 ¹⁰ 5x10 ¹⁰	3.19x10 ¹¹ 8.42x10 ¹⁰	3.87x10 ² 3.19x10 ¹ *	<ul style="list-style-type: none"> - Increase in dark current - No change in U_{bd}

* According to our calculations that depends on deducing the stopping power value of protons, with energy stated in the reference, in Si lattice, from the NIST database, and using the stated integrated flux, the dose value of this measurement must be ~ 7.88x10¹ Gy.

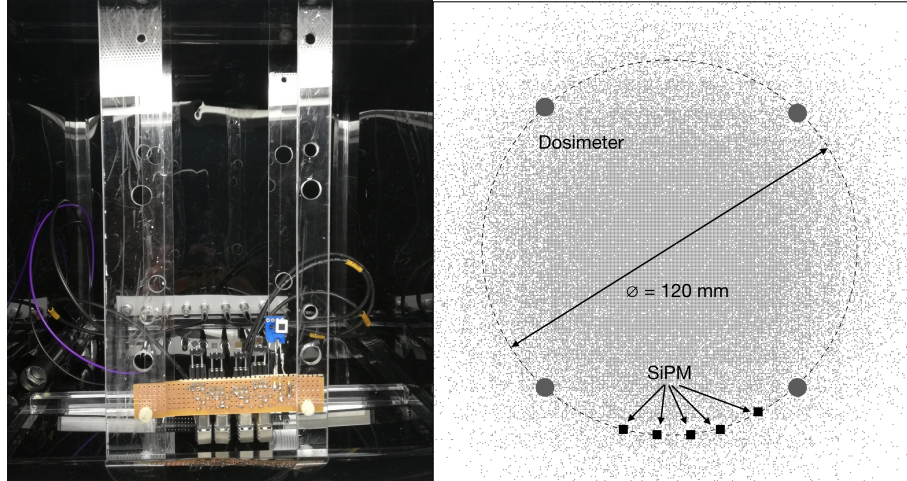


Figure 1: Arrangement of the SiPMs in the irradiation box (left), positioned at 6 cm from the center of the beam axis, with four dosimeters as shown in the sketch on the (right). In the photo on the left side the dosimeters were not mounted.

2 Instrumentation

2.1 The Test Setup

Figure 1 shows a picture (left) with a sketch (right) of the radiation test station located at the Institut für Kernphysik (IKP), Forschungszentrum Jülich, Germany. The proton beam produced by the JULIC cyclotron [15], with energy ~ 35 MeV, was defocused covering an area of about 20 cm diameter in order to reduce the particle rate. The SiPMs were mounted in a closed light-tight box at a radius of 6 cm from the the beam center in order to reduce the dose variation due to position uncertainty. The arrangement is sketched in Figure 1 (right). The beam has a gaussian profile as a function of the distance from the axis. For the dose measurement, 4 calibrated Farmer chamber dosimeters [16] were installed in addition at the same distance from the beam axis. Before installing the SiPMs, the beam was centered by adjusting the dose rates on the dosimeters to a comparable level resulting in an equal dose seen by the SiPMs. The sensitive volume of a dosimeter is 0.6 cm^3 with a sensitivity of 20 nC/Gy. Every second the accumulated charge is measured in each dosimeter by which the beam position and intensity is monitored during the irradiation. The area covered by a dosimeter was comparable to the area covered by a SiPM resulting in a comparable mean dose rate. The absolute dose measurement error was below 10%. The stability of the temperature inside the irradiation box was monitored by a DALLAS DS18B20 programmable resolution 1-wire digital temperature sensor controlled with a micro controller board "Arduino UNO control board" [17].

2.2 The Photo-Sensors

In this study five SiPM devices of interest to the $\bar{\text{P}}\text{ANDA}$ barrel-ToF detector were tested: two from KETEK [18] (PM3315-WB-BO and PM3325-WB-BO), one from Hamamatsu [19] (S13360-3050CS), SensL [20] (MicroFC-30035-SMT) and AdvanSiD [21] (ASD-NUV3S-P-40). Detailed information for each device is given in Table 2.

Table 2: Characteristics of the SiPM devices used in this study.

Device	Dimensions [mm ²]	Fill factor [%]	Breakdown voltage (U_{bd}) @22 °C	Over voltage (U_{ov})	Microcell size [μ m]
KETEK-15 μ m	3 x 3	65	27.5 V	4.0 V	15
KETEK-25 μ m	3 x 3	65	26.5 V	4.2 V	25
Hamamatsu	3 x 3	74	54.8 V	4.1 V	50
SensL	3 x 3	64	26.0 V	3.8 V	35
AdvanSiD	3 x 3	60	28.1 V	4.2 V	40

The contacting of the SiPMs was done by soldering pins at the anode and cathode, which were connected to 50 Ω coax cables with LEMO plugs. The operating bias of the SiPMs (and the preamplifier) was supplied by a TTI QL564T power supply [22].

2.3 The Data Acquisition (DAQ) System and Data Collection

The corresponding electronic circuit for the readout is shown Figure 2. The SiPMs were operated at 21 ± 0.2 °C and U_{ov} of ~ 4 V. The SiPM output signals were passed to a KETEK PEVAL-KIT MCX preamplifier unit [23], resulting in signals height amplification in the range of 5–10 mV for a single photon. The preamplified signals from the SiPMs were digitized by a 4–channel CAEN DT5720B digitizer unit [24] with 12 bit resolution, 2 V dynamic range, and a maximum sampling rate of 250 MHz. The captured pulses were sent to a PC and recorded by the DAQ CAEN Multi-PARAMeter Spectroscopy Software (CoMPASS) [25] for further off-line processing with ROOT [26].

Before irradiation, each SiPM was separately tested for its performance. In order to reduce the noise level, the irradiation box and the preamplifier were placed in an aluminum box that was equipped with feedthroughs for power supplies and signal. In this configuration a noise level of the amplified signal of ~ 2 mV could be achieved, which was sufficiently low for a clear separation of the single photon signals from the background. Therefore the signals from the SiPMs were acquired by setting a 4–5 mV threshold on the SiPM output signal amplitude in the discriminator node of the CoMPASS program. The digitizer acquisition time window was set to 4 μ s, with a sampling rate of 250×10^6 samples per second (MS/s) the waveforms were integrated over a fixed time window of 1 μ s after the trigger to obtain the collected charge of the event.

3 Data Analysis

The analysis strategy used in this experiment was similar to that explained in detail in [1]. The offline analysis first discriminates light signals from noise using a pulse finding algorithm (PFA), then calculates the total charge, Q_{tot} , collected by the SiPMs, for each event. The PFA selects signal pulses using a series of cuts. It first sets a lower limit on the pulse amplitude above the baseline. It then looks at the correlation between the pulse width and the corresponding integrated charge, as a 2D histogram. A ROOT graphical cut is used in this 2D plot to select and exclude the false signals and noise pulses with low charge and/or small width. The signal selection and noise rejection

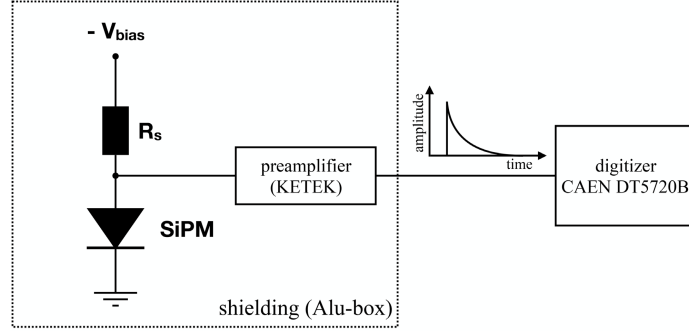


Figure 2: Schematics of the readout electronics. For the measurements the SiPM and preamplifier were placed for shielding in an aluminum-box (indicated by the dotted line.)

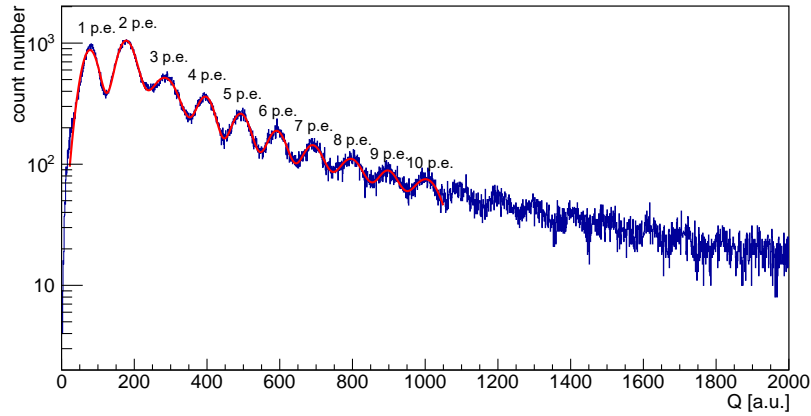


Figure 3: An example of the output charge spectrum of the AdvanSiD SiPM, taken in the dark, before exposure. The multi p.e. peaks are fitted with a sum of independent Gaussian functions (red line).

efficiency of the cuts are measured from the individual spectrum of each cut. The total charge for each identified signal is calculated by integrating the total ADC values in the pulse after baseline subtraction. The baseline is defined as the average of the waveform in the 19 ns time window prior to the trigger. Figure 3 shows an example of the output charge spectrum, taken in the dark, for the AdvanSiD SiPM (before radiation exposure), where each peak above zero corresponds to a quantized number of photoelectrons, p.e. The multi p.e. peaks are fitted with a sum of independent Gaussian functions to estimate the gain.

For the radiation hardness measurements the irradiation box was placed at the beam line but outside of the aluminum box, which led to a drastic increase in the noise level. Therefore, it was planned to conduct the irradiation test in several steps, with measurements in between. In view of the information available about the acceptable dose rates from the existing measurements, we planned for five steps of irradiation with a total dose of 50 Gy (corresponding to an integrated proton flux of $\phi_P=1.2 \times 10^{10}$ p/cm² and neutron equivalent fluence of $\phi_{n-eq}=2.45 \times 10^{10}$ n_{eq}/cm²) in each step. But already after the first irradiation step, all SiPMs seemed to be completely insensitive to detect light at the single photoelectron level. The noise was increased to a level of about 100 mV

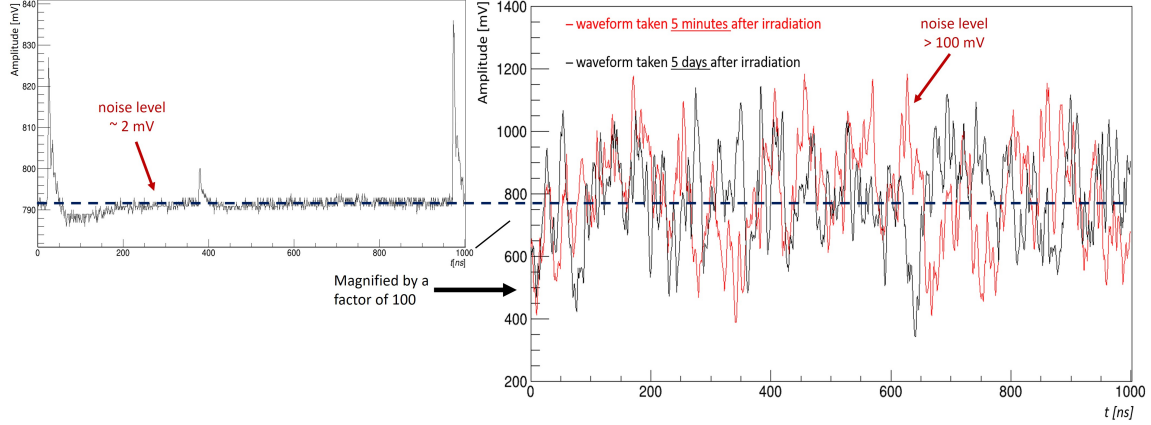


Figure 4: Typical signals of the SiPMs before (left side) and after (right side) irradiation with an integrated dose of 10 Gy. The level as well as the width of the noise band is drastically increased.

compared to the 2 mV before irradiation, as shown in Fig. 4. The typical signals of the SiPMs before irradiation were well separated and far above background with a reasonable signal rate (Fig. 4 (left)). The signal structure after irradiation confirms the drastic increase of the dark current with an drastically increased dark signal rate (Fig. 4 (right)). In view of a signal height of ~ 20 mV for a single photon, the devices are not usable for sensitive measurements at a few photoelectrons level.

In view of these initial results, and in order to get an insight view of the devices performance, we analyzed the critical parameters of the SiPMs.

3.1 I-V Curve Studies

Because the SiPMs I-V curve can reveal subtle changes in their characteristics, we measured the I-V behaviour of each device before and after irradiation. All the measurements were taken in the dark. In this measurement, each SiPM was connected to a picoammeter (Keithley 6485 [27]) and its leakage current as a function of the bias voltage was measured. The bias voltage was incremented in steps of 0.5 V up to $U_{bias} = 20$ V, after which the step size was reduced to 0.1 V up to ~ 6 V above the U_{bd} , to improve the accuracy of the breakdown voltage determination. The effective resolution of the system was dominated by noise pickup, which was on the order of 100 pA. Figure 5 shows the I-V curves for the five types of SiPMs, measured in the dark. The onset of breakdown is clearly visible in all SiPMs before irradiation (black markers). After irradiation the behavior drastically changed. A kind of avalanche effect, e.g. a strong current increase at a certain voltage, is still visible but the breakdown voltage is shifted to lower values, by ~ 2 V, in all cases. Furthermore the slope of the dark current increased by approximately 2 orders of magnitude.

3.2 SiPM Performance with Light

A test of the irradiated SiPMs sensitivity to photoelectrons was performed using light pulses from a laser diode. For this measurement, two SiPMs from AdvanSiD were used; an irradiated one (with an integrated dose of 1 Gy) and a new one of the same type. Both devices were illuminated by a pulsed blue laser diode and operated at the same bias voltage. The measurements were done by placing the SiPMs alternately at the same position while keeping the light system unchanged to achieve

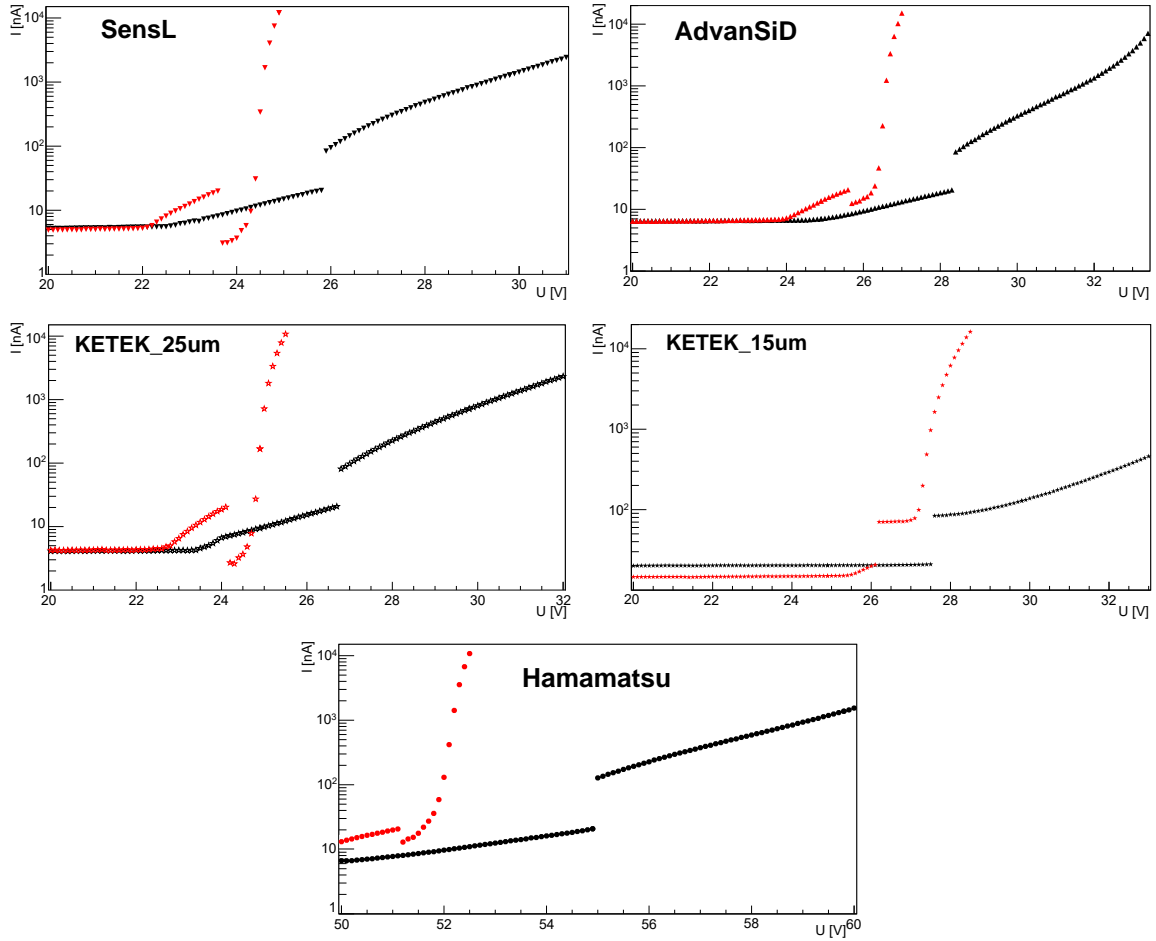


Figure 5: I-V curves before (black symbols) and after (red symbols) irradiation for SensL (top-left), AdvanSiD (top-right), KETEK-25 μm (middle-left), KETEK-15 μm (middle-right) and Hamamatsu (bottom) SiPMs.

the same illumination. The output signals from both SiPMs were captured and the total charges were compared. Figure 6, shows the corresponding output charge spectrum for both devices. The irradiated SiPM (lower plot) remained sensitive to the light source at the high p.e. level. However, multi-p.e. signals are not separable any more. The large increase in the gain of the irradiated SiPM (lower plot), compared to that with no irradiation (upper plot), is due to the fact that both devices were operated at the same operating voltage. Because, for the irradiated SiPM, the U_{bd} is reduced, as explained in section 3.1, the real applied U_{ov} is then increased, hence resulted in increasing the gain of this device.

3.3 SiPMs Visual Inspection

A visual inspection of the irradiated SiPMs was carried out at the end of the tests using an optical microscope, with magnification power ranging from 20x to 128x. The surfaces of the devices were carefully inspected, and photographs of specific locations were taken, before and after the irradiation tests. No visible evidence for damage was found on the outer surface of the SiPMs or at

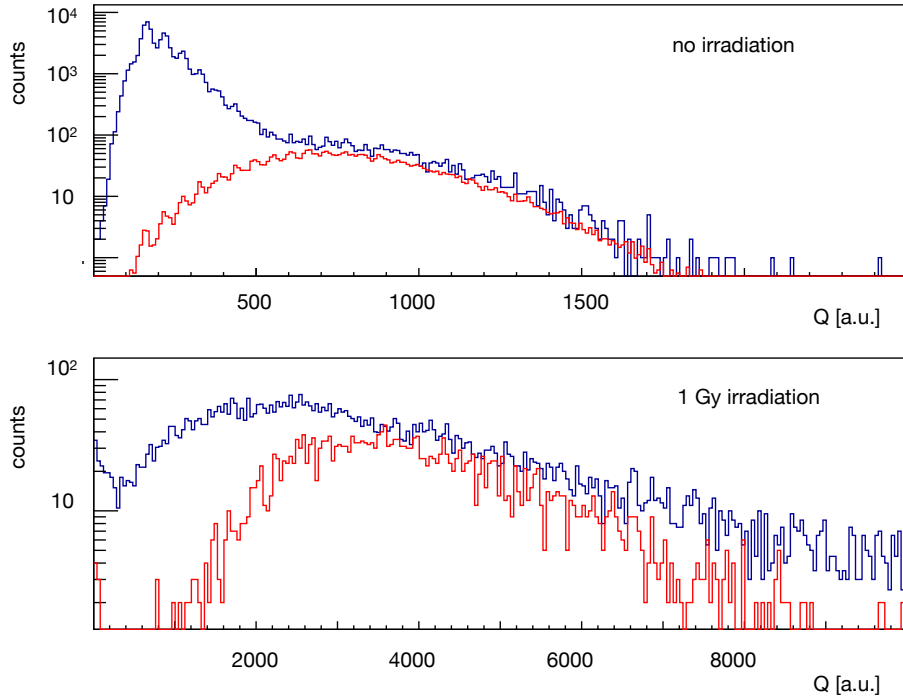


Figure 6: Comparison of a new "not-irradiated" AdvanSid SiPM (upper plot) and an irradiated one, with 1 Gy integration dose (lower plot). The SiPMs were illuminated by the same light pulses with a mean of about 12 photoelectrons. The blue curve results from selftriggering, while the signals of the red curves were triggered by the light pulse. After irradiation the background level is much higher and no single p.e. peaks are visible, however an external trigger allows to separate the light induced signals from the background distribution. The large increase in the gain in the irradiated device is due to the fact that both SiPMs were operated at the same voltage, but for the irradiated SiPM the U_{bd} is reduced, hence the real applied U_{ov} was increased.

the microcell level.

4 Data Taking During Irradiation

In order to follow the radiation damage as a function of the dose rate, an additional measurement was performed with one SiPM (the AdvanSiD) during irradiation. The dark current rate, gain, prompt cross-talk and correlated noise probabilities were studied at different doses and compared to their values in the absence of radiation exposure. To reduce the noise level, the irradiation box that houses the SiPM was shielded by a layer of aluminum foil, while the preamplifier was placed at a distance of about 2 m from the irradiation box, in a separate metal box. With these measures a noise level of about 3 mV was achieved. Furthermore, the cyclotron beam current was reduced to a dose rate of 0.001 Gy/s.

The development of the radiation damage can be observed in the signal charge spectra for a short time range with increasing radiation dose. Figure 7 shows the signal charge distributions,

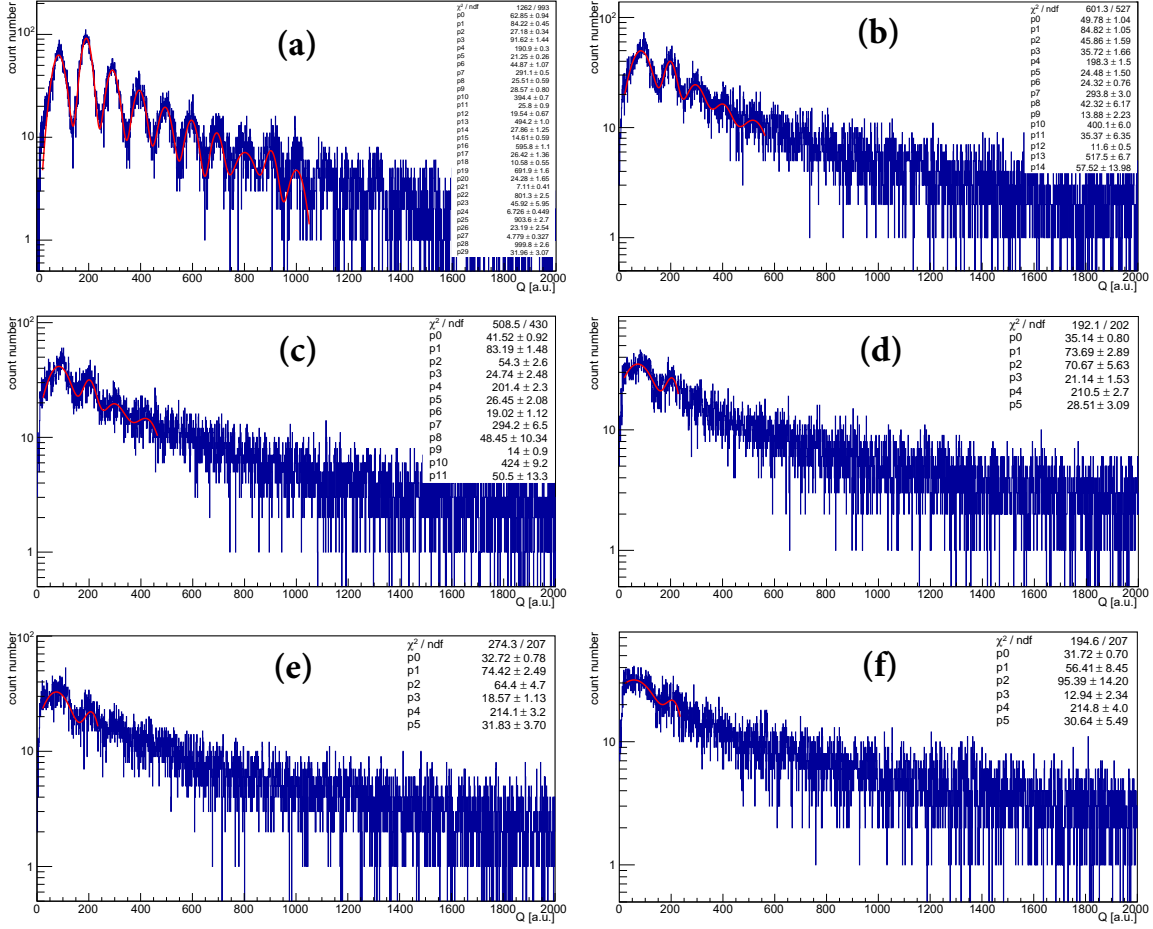


Figure 7: Signal charge distribution, taken in the dark, for the time intervals indicated in the integrated dose plot in Figure 8. For low radiation levels (distributions (a),(b),(c)) the photoelectron peaks up to 4 p.e. are clearly separated. At higher integrated dose the p.e. peaks start to get smeared. In the distribution (f) 2 p.e. are hardly resolved.

taken in the dark, for 10 s time intervals indicated in the integrated dose plot in Figure 8. The damage of the SiPM starts already at rather low integrated dose, of ~ 0.2 Gy.

Since this study mostly involves relative measurements, systematic effects that are independent of the radiation exposure cancel out. For the gain measurements, the total uncertainty is dominated by the systematic uncertainty related to changes in electronics pickup. To estimate this uncertainty we measured the FWHM of the baseline variations at the different dose values. We found at most $\sim 80\%$ deviation (at the highest dose value), for widths measured at non-zero radiation dose compared to that in the absence of exposure. This baseline noise was then added to simulated signal pulses to estimate its effect on the total charge calculation. This Monte Carlo study indicates that the extra noise pickup can lead to systematic errors in the measurement of the gain by the PFA of up to 8%. The statistical uncertainty for the gain measurement was found to be negligible. The correlated noise and the dark current rate, on the other hand, are limited by statistical uncertainties.

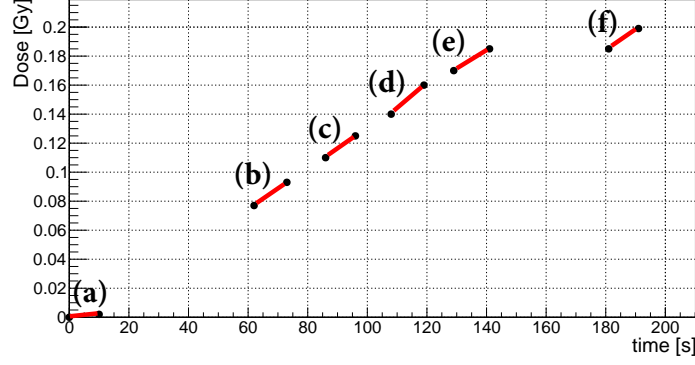


Figure 8: Integrated dose as a function of exposure time.

4.1 Relative Gain

The gain of a SiPM can be defined as the mean number of output electrons in the single p.e. peak. We used the charge distribution of the prompt signal, in Figure 7, to study the relative stability in the gain of the SiPM at different integrated dose values D . The mean value of each individual fitted Gaussian is used to estimate the average charge of the corresponding number of photoelectrons, $Q_{n\ p.e.}(D)$. The slope of the $Q_{n\ p.e.}(D)$ values, when plotted against the number of photoelectrons n , is then used to calculate the average charge of the SiPM single p.e. peak response at a specific D , $\bar{Q}(D)$. Thus the stability of the SiPM gain at different radiation doses can be assessed by the ratio, η_{Gain} , of the charge amplitude, $\bar{Q}(D)$ to that in the absence of the exposure:

$$\eta_{Gain} = \frac{\bar{Q}(D)}{\bar{Q}(D=0)} \quad (4.1)$$

Figure 9 (I) shows that the relative gain of the AdvanSiD SiPM stays constant as a function of the dose values until it reduces by $\sim 13\%$ at measurement (f), compared to that before irradiation.

4.2 Relative Dark Current Rate

SiPM dark current signals are mainly caused by thermally generated free charge carriers inside the avalanche region. The pulse of dark noise is similar to that triggered by a photon event. The dark current rate (DCR) is then defined by the rate of the SiPM output pulses, in dark, with amplitude level ≥ 1 p.e., and can be calculated by the following relation:

$$DCR = \frac{N_{\geq 1\ p.e.}}{t_{daq} \cdot A} \quad (4.2)$$

where $N_{\geq 1\ p.e.}$ is the number of the prompt signals with a measured charge of at least 1 p.e. amplitude level, t_{daq} is the data acquisition time window in seconds, and A is the surface area of the SiPM.

Figure 9 (II) shows η_{DCR} , the ratio of $DCR(D)$ to $DCR(D=0)$, as a function of the integrated dose. η_{DCR} shows a huge increase, by $\sim 30\%$ already during the first exposure measurement compared to its value with no exposure. Then it stays constant over the irradiation period.

4.3 Prompt Cross-Talk Probability

Correlated signals are an important source of noise in SiPMs. They are composed of prompt optical cross-talk and delayed after-pulses. The delayed correlated noise probability is discussed in section 4.4. The origin of prompt cross-talk can be understood as follows: when undergoing an avalanche, carriers near the p-n junction emit photons, due to the scattering of the accelerated electrons. These photons tend to be at near infrared wavelengths and can travel substantial distances through the device, including to neighboring microcells where they may initiate secondary Geiger avalanches. As a consequence, a single primary photon may generate signals equivalent to two or more photoelectrons. The prompt cross-talk probability, P_{CT} , depends on over-voltage, U_{ov} , which is the excess bias beyond the breakdown voltage, device-dependent barriers for photons (trenches), and the size of the microcells. The probability of prompt cross-talk can be calculated as:

$$P_{CT} = \frac{N_{>1 p.e.}}{N_{total}} \quad (4.3)$$

where $N_{>1 p.e.}$ is the number of the prompt signals with a measured charge of at least 1.5 p.e., and N_{total} is the total number of prompt signals above noise. Figure 9 (III) shows $\eta_{P_{CT}}$, the ratio of $P_{CT}(D)$ to $P_{CT}(D = 0)$, as a function of the integrated dose. $\eta_{P_{CT}}$ does not show a dependence on the dose values for measurements a, within the estimated uncertainties, while starting from measurements b to f it reduced by $\sim 6\%$, compared to the value in the absence of exposure.

4.4 Delayed Correlated Noise Probability

Both after-pulsing and delayed cross-talk events originate from an existing pulse. After-pulsing is due to the carriers trapped in silicon defects during the avalanche multiplication, then released later during the recharge phase of the microcell. Delayed cross-talk is generated by a similar mechanism to prompt cross-talk. The difference is that the photons generated during the avalanche process are absorbed in the inactive regions of the neighboring cells instead. It takes some time for the minority charge carriers to diffuse into the active region, causing a delayed signal. In our measurement, we cannot separate after-pulsing from delayed cross-talk and we count them together as delayed correlated noise.

To estimate the delayed correlated noise probability, P_{CN} , we count the number, N , of clearly separated pulses occurring immediately after the primary pulse. The time window used for the pulses integration is limited by the acquisition window. The primary pulse time window is found to be ~ 15 ns. P_{CN} is then estimated by normalizing N to the total number of events that contain prompt signals, N_{prompt} :

$$P_{CN} = \frac{N}{N_{prompt}} \quad (4.4)$$

Figure 9 (IV) shows $\eta_{P_{CN}}$ as a function of the integrated dose. It shows a constant response for the low dose measurement (a), while it increased by $\sim 30\%$ to $\sim 40\%$ for measurements (b) to (f), compared to the value in the absence of exposure.

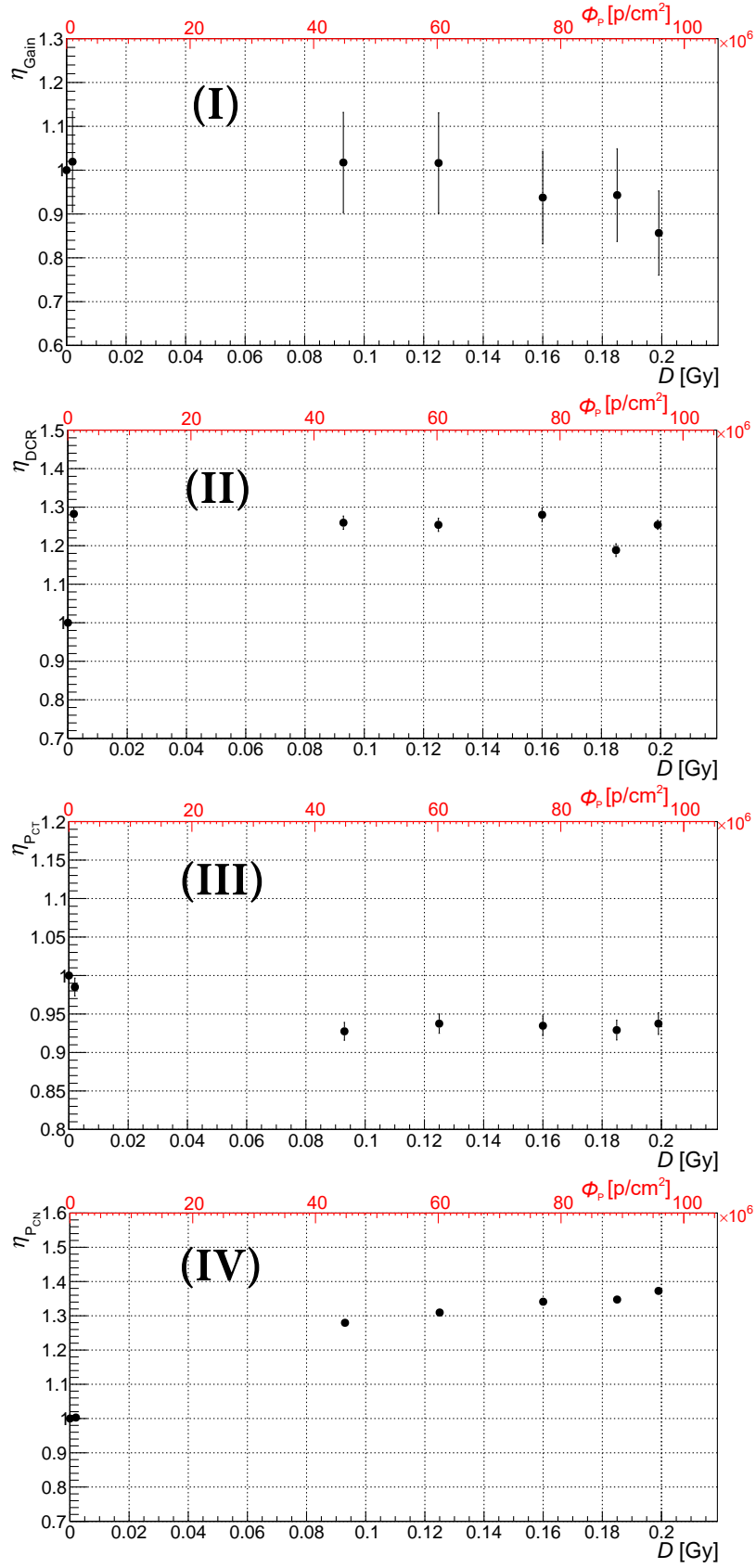


Figure 9: The relative gain (I), DCR (II), the prompt CT-probability (III) and the delayed correlated noise (IV) as a function of radiation dose (bottom x-axis) and proton flux (top x-axis).

5 Conclusions

The radiation hardness of the photosensors is an important characteristic that needs to be carefully studied, especially for those devices that will have long exposure time. Due to the increased use of SiPMs as photosensors the effect of radiation exposure on their performance is a mandatory investigation. A large number of studies in this field are already available with the general feature of an increased dark current. However, the usability of SiPMs as a function of radiation dose is not well defined due to the manufacturer dependent variation of the detailed structure and the large differences in the detected signals.

Based on available data, a rather high tolerable radiation level was expected, but already at a very low integrated dose drastic effects on the signal were observed. A dose of only 0.2 Gy was sufficient to result in a drastic increase of the dark current and a complete dissolution of separate photoelectron peaks. The use of such sensors, the SiPMs, as a standalone single photon detector is nearly impossible due to the high dark count rate if a certain radiation level is expected. But even the exposure to rather high integrated dose doesn't destroy the SiPMs completely. The functionality as photosensor with avalanche behavior at higher light signals, is maintained and a triggered readout can separate the signal to be measured from the dark counts. In all irradiated SiPMs in our analysis we identified a clear reduction of the breakdown voltage by up to about 2 V, resulting in much higher signals and dark count rate when operating at a fixed operating voltage. This effect should be considered by lowering the voltage to operate the device at a fixed over-voltage rather than a fixed operating voltage. A detailed knowledge of the SiPM damage induced by radiation requires more careful studies with devices with a well known internal structure to disentangle the influence of relevant parameters.

These irradiation studies are a first step of SiPM radiation hardness investigations and will be continued with higher proton energies close to the minimum ionizing region, which is more relevant for the typical scintillator readout in particle detectors.

Acknowledgments

We thank the crew of the JULIC cyclotron at the Nuclear Physics Institute at Forschungszentrum Jülich GmbH for the delivery of the well defined low intensity cyclotron beam and the precise determination of the applied dose rate. This work has been in part funded by the Deutsche Forschungsgemeinschaft (DFG, German Research Foundation) - Projektnummer 423761110.

References

- [1] X. Sun et al., *Study of Silicon Photomultiplier Performance in External Electric Fields*, *Journal of Instrumentation* **13** (2018) T09006.
- [2] \bar{P} ANDA-Collaboration, “*Technical Design Report for the: \bar{P} ANDA Barrel Time-of-Flight.*” https://panda.gsi.de/system/files/user_uploads/ken.suzuki/RE-TDR-2016-003_0.pdf, 2018.
- [3] \bar{P} ANDA-Collaboration, “*Technical Progress Report, FAIR-ESAC/Pbar.*” https://panda.gsi.de/oldwww/archive/public/panda_tpr.pdf, 2005.

- [4] M. Huhtinen and P. Aarnio, *Pion induced displacement damage in silicon devices*, *Nuclear Instruments and Methods in Physics Research Section A: Accelerators, Spectrometers, Detectors and Associated Equipment* **335** (1993) 580 – 582.
- [5] Gianluigi Casse, PhD thesis, “*The effect of hadron irradiation on the electrical properties of particle detectors made from various silicon materials.*” <http://hep.ph.liv.ac.uk/~gcasse/home.htm>, 1998.
- [6] A. H. Heering et al., *Radiation Damage Studies on SiPMs for Calorimetry at the Super LHC*, in 2008 *IEEE Nuclear Science Symposium Conference Record*, pp. 1523–1526, Oct, 2008. DOI.
- [7] Y. Musienko et al., *Study of Radiation Damage Induced by 82MeV Protons on Multi-Pixel Geiger-Mode Avalanche Photodiodes*, *Nuclear Instruments and Methods in Physics Research Section A: Accelerators, Spectrometers, Detectors and Associated Equipment* **610** (2009) 87 – 92.
- [8] P. Bohn et al., *Radiation Damage Studies of Silicon Photomultipliers*, *Nuclear Instruments and Methods in Physics Research Section A: Accelerators, Spectrometers, Detectors and Associated Equipment* **598** (2009) 722 – 736.
- [9] T. Matsumura et al., *Effects of Radiation Damage Caused by Proton Irradiation on Multi-Pixel Photon Counters (MPPCs)*, *Nuclear Instruments and Methods in Physics Research Section A: Accelerators, Spectrometers, Detectors and Associated Equipment* **603** (2009) 301 – 308.
- [10] Y. Musienko et al., *Radiation Damage Studies of Silicon Shotomultipliers for the CMS HCAL Phase I Upgrade*, *Nuclear Instruments and Methods in Physics Research Section A: Accelerators, Spectrometers, Detectors and Associated Equipment* **787** (2015) 319 – 322.
- [11] A. Heering et al., *Effects of Very High Radiation on SiPMs*, *Nuclear Instruments and Methods in Physics Research Section A: Accelerators, Spectrometers, Detectors and Associated Equipment* **824** (2016) 111 – 114.
- [12] K. Lacombe et al., *Impact of Proton Irradiation on SiPM Dark Current for High-Energy Space Instruments*, *JPS Conf. Proc.* **27**, 012006 (2019) .
- [13] E. Garutti and Y. Musienko, *Radiation damage of SiPMs*, *Nuclear Instruments and Methods in Physics Research Section A: Accelerators, Spectrometers, Detectors and Associated Equipment* **926** (2019) 69 – 84.
- [14] B. Biroét al., *A Comparison of the Effects of Neutron and Gamma Radiation in Silicon Photomultipliers*, *IEEE Transactions on Nuclear Science* **66** (2019) 1833–1839.
- [15] W. Braeutigam et al., *Status and perspectives of the cyclotron JULIC as COSY injector*, *Nukleonika* **48** (2003) .
- [16] Farmer@Ionization Chambers 30010, PTW-Freiburg. <http://www.ptwdosimetry.com>.
- [17] ARDUINO. <https://www.arduino.cc/>.
- [18] KETEK. <https://www.ketek.net/sipm/>.
- [19] Hamamatsu. <http://www.hamamatsu.com>.
- [20] SensL, “*Technical Note: Introduction to SiPM.*” <http://www.sensl.com>.
- [21] AdvanSiD, “*Application note: Introduction to SiPMs.*” <http://advansid.com>.
- [22] Aim-TTi. <https://www.aimtti.com/>.
- [23] Ketek, “*Ketek Easy-to-use SiPM Evaluation Kits with Preamplifier Data Sheet.*” https://www.aptechnologies.co.uk/images/Data/Ketek/DS_SiPM-Evaluation-Kit.pdf.

- [24] CAEN, “DT5720B Digitizer Data Sheet.” <http://www.caen.it>.
- [25] CAEN, “Compass.” <https://www.caen.it/products/compass>.
- [26] R. Brun and F. Rademakers, *ROOT - An object oriented data analysis framework*, *NIM A389* (1997) 81 – 86.
- [27] Keithley. <http://www.keithley.com>.